Short Communication

Capacitive Nanosized Spinel α-LiFe₅O₈ as High Performance Cathodes for Lithium-ion Batteries

Wei Zhou, Yourong Wang[*], *Liping Zhang, Guangsen Song and Siqing Cheng*[*]

Innovation Center for Nanomaterials in Energy and Medicine (ICNEM), School of Chemical and Environmental Engineering, Wuhan Polytechnic University, Hubei 430023, P. R. China
[*]E-mail: icnem@hotmail.com

The nanosized spinel α-LiFe₅O₈ with a grain size of about 10 nm was fabricated by a facile solid state method via the assistance of oxalic acid. The as-prepared α-LiFe₅O₈ electrode for lithium ion battery delivers a high reversible initial specific capacity of 257.1 mA h g^{-1} at 28 mA g^{-1} and remaining at 130 mAh g^{-1} at as high as 2820 mA g^{-1} even after 100 cycles, as well as excellent rate capability and improved cycling stability, which has not reported before for lithium ferrite oxides. This might be attributed to the characteristic pseudocapacitive behavior of lithium storage in nanosized spinel α-LiFe₅O₈ and the structural stability of α-LiFe₅O₈ upon charge/discharge as well, as evidenced by CV measurement for the as-prepared α-LiFe₅O₈ electrode. The unique combination of those features for lithium ion battery and capacitor is potential to develop high performance hybrid energy storage device for the needs of electric vehicle batteries and other high powder applications.

1. INTRODUCTION

Considerable attention has been focused on the family of lithium iron oxide compounds for potentially attractive alternative as cathode materials in rechargeable lithium ion secondary battery given the low cost, most abundance, thermally safety and environmentally benign of iron[1-3], although LiCoO₂ is still being used as a successful cathode material in most commercial lithium-ion batteries[1]. The simplest compound of this family is LiFeO₂ with a theoretical capacity of 282 mA h g^{-1} and thus investigated extensively as electrode hosts[3-7]. However, it seems to be very difficult to improve the cycling stability and rate capability of LiFeO₂ owing to its quite complex polymorphism and intrinsic charge/discharge mechanism[8-10] despite the up-to-date reported best α-LiFeO₂–C composite with the discharge capacity of 230 mA h g^{-1} at 0.5 C after 100 cycles[11]. It has been

persuaded strongly[10] that orthorhombic $LiFeO_2$ undergoes a structural change to spinel phase $LiFe_5O_8$ during the charge/discharge process, which results in the capacity fading of the $Li/LiFeO_2$ system, as similar in the orthorhombic $Li/LiMnO_2$ system for the capacity loss mechanism of the $Li/LiMnO_2$ cell due to the conversion from the orthorhombic to spinel structure[12-14]. As such, the orthorhombic $LiFeO_2$ appears to essentially exhibit irreversible capacity however it is improved due to the phase transformation upon charge/discharge. Inspired by that, we assume that the structurally stable spinel $LiFe_5O_8$, when used as cathode for lithium ion battery instead of $LiFeO_2$, should be more able to present a reversible capacity.

The spinel $LiFe_5O_8$ is known to crystallize in two polymorphic modifications (α, β) depending on the synthesis and processing procedures and mostly it is investigated for fundamental physical phenomena proceeding in materials based on $LiFe_5O_8$.[15] Thus, the synthesis of the spinel $LiFe_5O_8$ in most practical applications, in particular, with nanostructured $LiFe_5O_8$ was explored extensively using different starting materials via various methods at low temperature such as coprecipitation, sol-gel method, hydrothermal method, etc.[16-19] However, it is less concern for spinel $LiFe_5O_8$ to be employed as cathode materials in rechargeable lithium batteries except for some reported mixed phase materials containing $LiFe_5O_8$ compared with electrochemically active $LiFeO_2$. Typically, Kim and Manthiram[20] reported the nano-crystalline lithium iron oxide ($Li_xFe_yO_z$) containing $LiFe_5O_8$ with a discharge capacity of about 140 mA h g^{-1} in the range of 1.5–4.3V, exhibiting a good cyclability. Likewise, Lee et al[21] also prepared the nano-crystalline lithium iron oxide ($Li_xFe_yO_z$) composed of α-$LiFe_5O_8$, β-$LiFe_5O_8$, and a trace of cubic α-$LiFeO_2$ to deliver an initial discharge capacity of 215 mA h g^{-1} with excellent cycling retention. Nevertheless, the spinel $LiFe_5O_8$ shows potential as cathode material for lithium ion battery with high rate capability and good cycling stability because lithium could be intercalated/deintercalated reversibly in and out of $LiFe_5O_8$.[22] Herein, we presented a facile solid state synthesis of nanocrystalline α-$LiFe_5O_8$ assisted by oxalic acid at low temperature and found for the first time that the as-prepared α-$LiFe_5O_8$ as cathode material for lithium ion secondary battery renders pseudocapacitive character, thus exhibiting high rate capability and excellent cycleability, specially at a fairly high discharge current density.

2. EXPERIMENTAL SECTION

Lithium iron oxides were synthesized from $LiOH \cdot H_2O$ (Changzhou Chenhua Chemicals, 95.0%), $LiNO_3$ (Tianjin Kemiou Chemical Reagent, 99.0 %), $Fe(NO_3)_3 \cdot 9H_2O$ (Tianjin Baishi Chemicals, 98.5%) and oxalic acid (Tianjin Baishi Chemicals, 99.0%) by a solid-state method. Stoichiometric amounts of the starting materials were thoroughly ground in a mortar with a pestle for 2 h. The mixture was calcined in a box furnace in air at 250 ℃ for 3 h. the as-obtained solid product was collected, washed repeatedly with distilled water, ethanol, and dried at 80℃ under vacuum, and then calcined at 600 ℃ for another 3 h.

Powder X-ray diffraction (XRD-6000, Shimadzu, Japan) using Cu Kα radiation (λ = 1.5418 Å) at a scanning step of 2° per minute was used to identify the crystalline phase of the as-prepared lithium iron oxides. The particle size and morphology of the compounds were observed with a field emission

scanning electron microscopy (FE-SEM, Hitachi, Japan) and transmission electron microscope (TEM, JEOL-2010, Japan) with an accelerating voltage of 200 kV. The Fourier transform infrared (FT-IR) spectroscopic measurements were carried on a NEXUS671 spectrometer using the KBr pellet technique.

The positive electrodes were fabricated by pasting the slurries of the as-prepared lithium iron oxide powder (70 wt%), acetylene black (20 wt%), and polyvinylidene difluoride (PVDF, 10 wt%) dissolved in N-methylpyrrolidone (NMP) on Al foil strips by the doctor blade technique. Then the strips were dried at 80℃ for 24 h in an air oven to remove water molecules. The electrolyte was 1 M $LiPF_6$ in a mixture of ethylene carbonate (EC)/diethyl carbonate (DEC) (1:1 by volume), the separator was CelgardR 2325. 2016 coin-type cells were assembled in an Ar-filled glove box using lithium metal foil as the counter electrode. The measurements of electrochemical performance were carried out on a program-controlled Battery Test System (Land®, Wuhan, China) at room temperature. The cyclic voltammetry (CV) was conducted in a three-electrode cell with lithium foil as counter and reference electrodes by using a CHI660B Electrochemical Work-station (Chenghua, Shanghai, China) at room temperature.
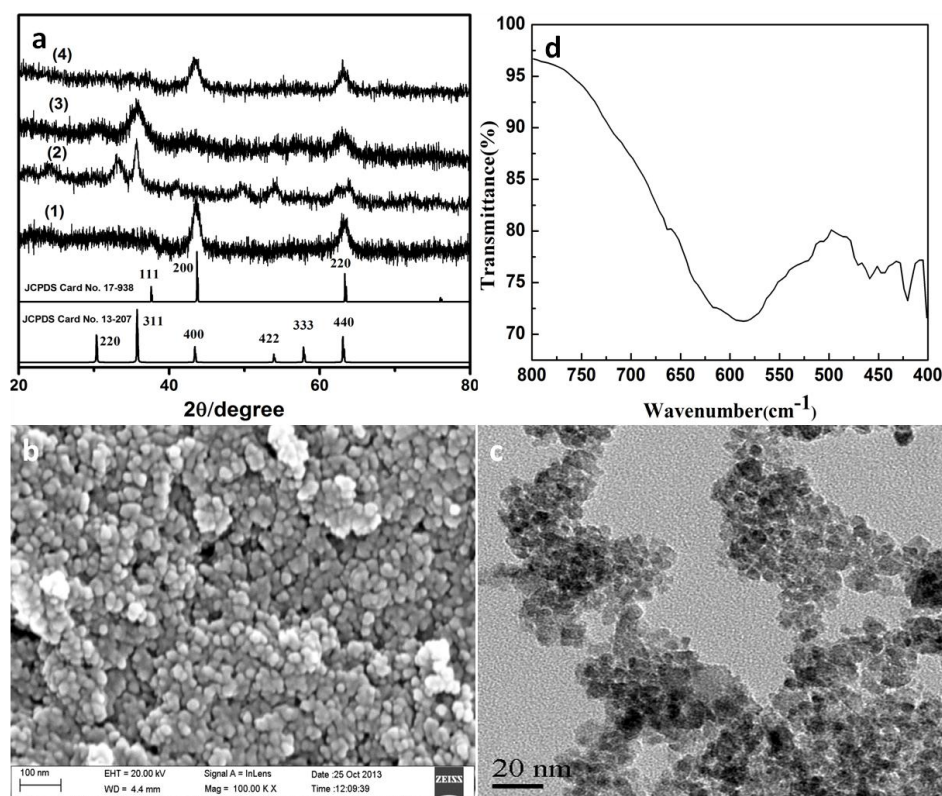
3. RESULTS AND DISCUSSION

Figure 1. (a) X-ray diffraction patterns of the obtained products at 250 ℃ with different oxalic acid concentration of (1) 0, (2) 30 wt%, (3) 60 wt%, (4) 90 wt%; (b) SEM image of the as-prepared α-LiFe$_5$O$_8$; (c) TEM image of the as-prepared α-LiFe$_5$O$_8$; (d) FT-IR of the as-prepared α-LiFe$_5$O$_8$.

Fig.1a presents the powder X-ray diffraction patterns of the as-prepared products at 250 ℃ with different oxalic acid concentration by a solid state method, showing the oxalic acid dependence of fabrication of α-LiFe$_5$O$_8$. Generally, the starting materials LiOH·H$_2$O, LiNO$_3$ and Fe (NO$_3$)$_3$·9H$_2$O are mixed fully in a mortar and sintered at 250 ℃ to yield pure phase nanocrystalline α-LiFeO$_2$ (Fig. 1a(1)), which was also indicated in our previous work[23]. However, in the presence of oxalic acid, the products obtained are various with oxalic acid concentration. When the weight percentage of oxalic acid is 30%, the mixed phase material containing α-LiFe$_5$O$_8$ is produced, as shown in Fig.1a(2). While the weight percentage of oxalic acid is increased up to 60%, the pure phase α-LiFe$_5$O$_8$ (Fig. 1a(3)) is obtained. With further increase of the weight percentage of oxalic acid up to 90%, the product seems to return to α-LiFeO$_2$ (Fig. 1a(4)). Oxalic acid is usually used to assist the syntheses of uniform nanosized lithium compounds at low temperature [24-26] because oxalic acid facilitates the well contact between reactants and the produced oxalate compound precursor has low decomposition temperature. As such, it is found that oxalic acid could not only assist the synthesis but also induce the transformation between different lithium ferrite oxides depending on oxalic acid concentration. Obviously, the spatial arrangement between Li and Fe and the ratio of Li/Fe in lithium ferrite oxide are relative to the amount of oxalate compound produced because oxalic acid concentration is the direct dependence of the amount of Li and Fe oxalate compound, which is similar to the proven temperature dependence of the spatial arrangement between Li and Fe and the ratio of Li/Fe in lithium ferrite oxides[27-28].

Hereby, we aim to mainly focus on the as-prepared α-LiFe$_5$O$_8$ used as cathode material for lithium ion battery. As shown in Fig.1a(3), All diffraction peaks can be easily indexed to a pure cubic phase (space group P4$_1$32[227]) of α-LiFe$_5$O$_8$ with lattice parameter a = 8.333 Å, which is close to the reported data for cubic α-LiFe$_5$O$_8$ (JCPDS Card No. 13-207),[29] indicating the formation of a single phase α-LiFe$_5$O$_8$. It is seen that all diffraction peaks exhibit broad reflection patterns, which shows an amorphous-like phase structure with poor crystallinity, small particle-size. According to Debye-Scherrer equation[30], the crystallite size of the as-prepared α-LiFe$_5$O$_8$ is evaluated from the most intense peak (311) to be ca. 10 nm, which is further corroborated by SEM (Fig. 1b) and TEM (Fig. 1c) images. Simple FT-IR spectroscopy of the as-prepared α-LiFe$_5$O$_8$ (Fig. 1d) shows two characteristic vibration bands in the range ～550–600 cm^{-1} and～430–490 cm^{-1}, corresponding to the formation of tetrahedral and octahedral clusters, respectively, and indicating the presence of M–O stretching band in ferrites, which is in agreement with the reported α-LiFe$_5$O$_8$. No vibration bands are observed at about 3000 cm^{-1} or 1500–1550 cm^{-1} (not shown here), which excludes the presence of trace impurities such as oxalate compound and Li$_2$CO$_3$ in the final product.

The electrochemical performances of the as-prepared α-LiFe$_5$O$_8$ nanoparticles were investigated using half cells *vs.* Li/Li$^+$ in the potential range 1.5-4.5 V, as shown in Fig. 2. Fig. 2a shows the galvanostatic charge-discharge curves of α-LiFe$_5$O$_8$ cells for the first three cycles at a current density of 28 mA g^{-1}. The first charge curve for the cell with α-LiFe$_5$O$_8$ obtained rapidly increases up to 4.1 V (inset of Fig.2a) and exhibits a voltage plateau between 4.2 and 4.3 V. For the subsequent two cycles, the charge curves tend to gradual decrease in voltage without any remarkable voltage plateau and exhibit slightly different shapes compared with that of the first cycle.
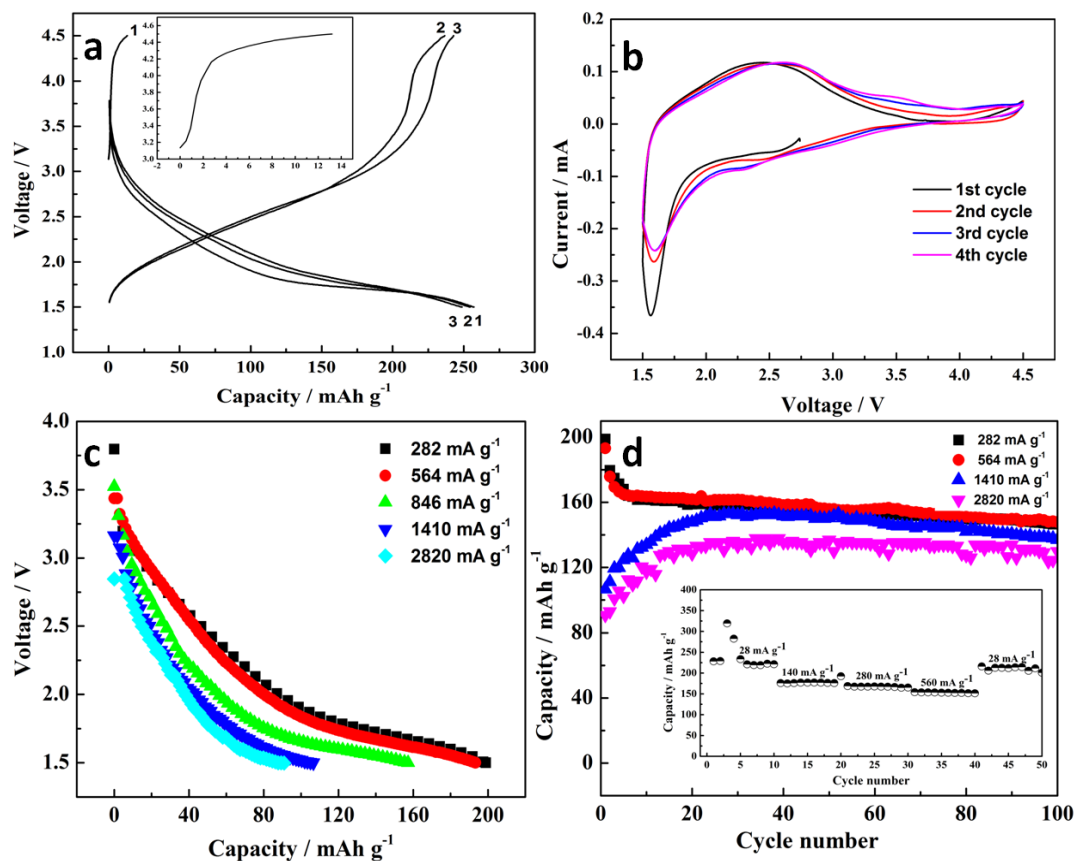
Figure 2. Electrochemical performance of the as-prepared α-LiFe$_5$O$_8$ as cathode material for lithium ion battery. (a) Galvanostatic charge-discharge curves for the first three cycles at 28 mA g^{-1}; (b) Cyclic voltammograms of the as-preparedα-LiFe$_5$O$_8$ electrode for the first three cycles at sweep rate of 0.2 mV s^{-1}; (c) Galvanostatic discharge curves at different current densities; (d) Cycling stability of the as-prepared α-LiFe$_5$O$_8$ cell at different current densities, inset: consecutive cycling behavior at different rates.

This could be attributed to the formation of solid electrolyte interface (SEI) film during the first charge.[31-32] However, all discharge curves for the cell with α-LiFe$_5$O$_8$ obtained drop rapidly to 3.0 V and then gradually reach a plateau of 2.0 V, and finally decreases down to 1.5 V. The reversible discharge capacities for the first three cycles at current density of 28 mA g^{-1} are 257.1, 254.5 and 248.7 mAh g^{-1}, respectively and no appreciable capacity loss is observed. Therefore, the as-prepared α-LiFe$_5$O$_8$ represents a good structural stability during charge/discharge when used as cathode material for lithium ion batteries and exhibits a potential cycling retention, which is further manifested by cyclic voltammetry (CV) of α-LiFe$_5$O$_8$ cell in the first three discharge-charge cycles at sweep rate of 0.2 mV s^{-1} (Fig.2b). There are two pairs of peaks in each CV. The observation of a pair of peaks located between 1.5 V and 1.6 V (denoted as A peak) are the characteristic pseudocapacitive behavior of lithium storage in LiFe$_5$O$_8$ [33] while another pair of peaks located between 2 V and 2.6 V (denoted as B peak) is the typical behavior expected for the oxidation state of iron switching between +3 and +2.6 due to lithium intercalation/deintercalation, corresponding to the reversible reaction: $(1/2)$LiFe$_5$O$_8$ + Li$^+$ ↔ $(1/2)$ Li$_3$Fe$_5$O$_8$. [22] Obviously, the peak current in peak A is much higher than that of peak

B, indicating the domination of lithium storage process over the redox reaction of iron. This phenomenon directly appears in the discharge-charge curves with different rates (Fig. 2c). In relative low rate (282, 564, 846 mA g^{-1}) discharge-charge curves, a distinct plateau appears at 2.0 V, corresponding to the redox reaction of iron due to lithium insertion/de-insertion. With the increase of charge-discharge rates, the plateau gradually diminishes, indicating that the as-prepared α-LiFe$_5$O$_8$ has the capability to maintain capacity by the pseudocapacitive process of lithium storage at high current rate. At 2820 mA g^{-1}, the discharge capacity for the as-prepared α-LiFe$_5$O$_8$ electrode still retains 92.4 mAh g^{-1}, which has never been reported before. On the other hand, the CV curves of the as-prepared α-LiFe$_5$O$_8$ electrode for the first three cycles almost overlap, except for the cathodic peak located between 1.5 V and 1.6 V due to the formation of SEI film, revealing a good reversibility. In order to test the cycling stability, a lithium cell made using the as-prepared α-LiFe$_5$O$_8$ was run at different rates. As shown in Fig. 2(d), the discharge capacity at 282 and 564 mA g^{-1} tends to decrease in the first several cycles and then almost keeps stable, the discharge capacity at the current density of 564 mA g^{-1} is 148 mAh g^{-1} after 100 cycles, which is approximately 76.6% of its initial discharge capacity. On contrary, at higher current densities of 1410 and 2820 mA g^{-1}, the discharge capacity firstly increases and then tends to be stable, the discharge capacity at current density of 2820 mA g^{-1} still maintains at as high as 130 mAh g^{-1} after 100 cycles. This could be attributed to the wetting process of the electrodes with the electrolytes prior to stabilization of the electrochemical reactions.[34-35] Furthermore, the rate performance of the as-prepared α-LiFe$_5$O$_8$ electrode at different charge/discharge rates, measured after 10 cycles at each rate from 28 to 560 mA g^{-1} in an ascending order, followed by a return to 28 mA g^{-1}, is shown in inset of Fig.2(d). The α-LiFe$_5$O$_8$ electrode presents excellent cycling stability at each rate, and reversible capacities were measured to be 221, 176, 168 and 154 mAh g^{-1} at the rate of 28, 140, 280 and 560 mA g^{-1}, respectively. After 50 cycles, the reversible capacity of the α-LiFe$_5$O$_8$ at 28 mA g^{-1} was still 211 mAh g^{-1} (95.5% of the initial reversible capacity of 221 mAh g^{-1}), illustrating its excellent cycling performance, even after cycling at relative high rates.

4. CONCLUSIONS

In summary, we fabricated and synthesized successfully the nanosized spinel α-LiFe$_5$O$_8$ with a grain size of about 10 nm by facile solid state method via the assistance of oxalic acid at low temperature, which was characterized clearly by XRD, SEM, TEM and FT-IR techniques. CV measurement for the as-prepared α-LiFe$_5$O$_8$ electrode for lithium ion battery showed that the α-LiFe$_5$O$_8$ is stable structurally upon discharge/charge and the pseudocapacitive lithium storage in nanosized spinel α-LiFe$_5$O$_8$ dominates the redox reaction of iron due to lithium insertion/de-insertion, indicating the promising cycling stability and high rate performance of the as-prepared α-LiFe$_5$O$_8$ cathode material for lithium ion battery. In addition, the nanosized spinel structure facilitates adequate electrode-electrolyte contact and electronic transport. The integration of these features enables this material to exhibit a remarkable energy density much high than the commercial sueprcapacitors, and can even compare with commercial lithium-ion batteries with improved power density, have superior lithium storage performance, which will be applicable to the development of high-performance

supercapacitor-battery hybrid energy storage device for electric vehicle batteries and other high powder applications.

References

1. J. B. Goodenough and K.-S. Park, *J. Am. Chem. Soc.* , 135(2013)1167.
2. Y. S. Lee, S. J. Cho, Y. K. Sun, K. Kobayakawa and Y. Sato, *Electrochemistry*, 73(2005)874.
3. P. C. Wang, H. P. Ding, T. Bark and C. H. Chen, *Electrochim Acta*, 52(2007)6650.
4. A. E. Abdel-Ghany, A. Mauger, H. Groult, K. Zaghib and C. M. Julien, *J. Power Sources* 197(2012)285.
5. K. Li, H. Chen, F. Shua, K. Chen and D. Xue, *Electrochim Acta*, 136(2014)10.
6. J. Morales and J. Santos-Peña, *Electrochem. Commun.* , 9(2007)2116.
7. Y. Wang, J. Wang, H. Liao, X. Qian, M. Wang, G. Song and S. Cheng, *RSC Adv*, 4(2014)3753.
8. Y. S. Lee, S. Sato, Y. K. Sun, K. Kobayakawa and Y. Sato, *J. Power Sources* 119-121(2003)285.
9. Y. S. Lee, S. Sato, M. Tabuchi, C. S. Yoon, Y. K. Sun, K. Kobayakawa and Y. Sato, *Electrochem. Commun.* , 5(2003)549.
10. J. Morales, J. Santos-Peña, R. Trócoli, S. Franger and E. Rodríguez-Castellón, *Electrochim Acta*, 53(2008)6366.
11. M. M. Rahman, J.-Z. Wang, M. F. Hassan, S. Chou, Z. Chen and H. K. Liu, *Energy Environ Sci*, 4(2011)952.
12. L. Croguennec, P. Deniard and R. Brec, *J. Electrochem. Soc.* , 144(1997)3323.
13. L. Croguennec, P. Deniard, R. Brec and A. Lecerf, *J. Mater. Chem.* , 5(1995)1919.
14. K. M. Shaju and P. G. Bruce, *Chem. Mater.* , 20(2008)5557.
15. A. P. Surzhikov, E. N. Lysenko, A. V. Malyshev, A. M. Pritulov and O. G. Kazakovskaya, *Russ Phys J*, 55(2012)672.
16. J. C. Anderson and M. Schieber, *J. Phys. Chem. Solids* 25(1964)961.
17. B. Li, Y. Xie, H. Su, Y. Qian and X. Liu, *Solid State Ionics* 120(1999)251.
18. M. Tabuchi, A. Nakashima, H. Shigemura, K. Ado, H. Kobayashi, H. Sakaebe, K. Tatsumi, H. Kageyama, T. Nakamura and R. Kanno, *J Mater Chem*, 131747.
19. S. Verma and P. A. Joy, *Mater. Res. Bull.* , 43(2008)3447.
20. J. Kim and A. Manthiram, *J. Electrochem. Soc.* , 146(1999)4371.
21. Y. T. Lee, C. S. Yoon, Y. S. Lee and Y.-K. Sun, *J. Power Sources* 134(2004)88.
22. M. Catti and M. Montero-Campillo, *J. Power Sources* 196(2011)3955.
23. J. Wang, Y. Wang, W. Zhou, X. Qian, M. Wang and S. Cheng, *Intl J Electrochem Sci*, 9(2014)3961.
24. H. Fang, L. Li and G. Li, *J. Power Sources* 167(2007)223.
25. T. Li, W. Qiu, G. Zhang, H. Zhao and J. Liu, *J. Power Sources* 174(2007)515.
26. Z. Zhu, H. Yan, D. Zhang, W. Li and Q. Lu, *J. Power Sources* 224(2013)13.
27. J. S. Baijal, S. Phanjoubam, D. Kothari, C. Prakash and P. Kishan, *Solid State Commun.* , 83(1992)679.
28. V. K. Sankaranarayanan, O. Prakash, R. P. Pant and M. Islam, *J. Magn. Magn. Mater.* , 252(2002)7.
29. W. S. Sheldrick and M. Wachhold, *Angew Chem Int Ed Engl*, 36(1997)206.
30. M. Anis-ur-Rehman, A. S. Saleemi and A. Abdullah, *J. Alloys Compd.* , 579(2013)450.
31. T. Muraliganth, A. Vadivel Murugan and A. Manthiram, *Chem. Commun.* , (2009)7360.

32. J. Su, M. Cao, L. Ren and C. Hu, *J Phys Chem C*, 115(2011)14469.
33. H. Liu, Z. Bi, X.-G. Sun, R. R. Unocic, M. P. Paranthaman, S. Dai and G. M. Brown, *Adv. Mater.* , 23(2011)3450.
34. C. J. Jafta, M. K. Mathe, N. Manyala, W. D. Roos and K. I. Ozoemena, *ACS Appl. Mat. Interfaces* 5(2013)7592.
35. J. Saint, A. S. Best, A. F. Hollenkamp, J. Kerr, J. H. Shin and M. M. Doeff, *J. Electrochem. Soc.* , 155(2008)A172.